THE JOURNAL OF BIOLOGICAL CHEMISTRY VOL. 286, NO. 14, pp. 12617–12626, April 8, 2011


# Deletion of the Distal C Terminus of $Ca_V1.2$ Channels Leads to Loss of $\beta$-Adrenergic Regulation and Heart Failure *in Vivo*[*]

Received for publication, August 13, 2010, and in revised form, December 30, 2010 Published, JBC Papers in Press, January 7, 2011, DOI 10.1074/jbc.M110.175307

**Ying Fu, Ruth E. Westenbroek, Frank H. Yu, John P. Clark III, Misty R. Marshall, Todd Scheuer, and William A. Catterall**[1]

*From the Department of Pharmacology, University of Washington, Seattle, Washington 98195-7280*

**L-type calcium currents conducted by $Ca_V1.2$ channels initiate excitation-contraction coupling in cardiac and vascular smooth muscle. In the heart, the distal portion of the C terminus (DCT) is proteolytically processed *in vivo* and serves as a noncovalently associated autoinhibitor of $Ca_V1.2$ channel activity. This autoinhibitory complex, with A-kinase anchoring protein-15 (AKAP15) bound to the DCT, is hypothesized to serve as the substrate for $\beta$-adrenergic regulation in the fight-or-flight response. Mice expressing $Ca_V1.2$ channels with the distal C terminus deleted ($DCT^{-/-}$) develop cardiac hypertrophy and die prematurely after E15. Cardiac hypertrophy and survival rate were improved by drug treatments that reduce peripheral vascular resistance and hypertension, consistent with the hypothesis that $Ca_V1.2$ hyperactivity in vascular smooth muscle causes hypertension, hypertrophy, and premature death. However, in contrast to expectation, L-type $Ca^{2+}$ currents in cardiac myocytes from $DCT^{-/-}$ mice were dramatically reduced due to decreased cell-surface expression of $Ca_V1.2$ protein, and the voltage dependence of activation and the kinetics of inactivation were altered. $Ca_V1.2$ channels in $DCT^{-/-}$ myocytes fail to respond to activation of adenylyl cyclase by forskolin, and the localized expression of AKAP15 is reduced. Therefore, we conclude that the DCT of $Ca_V1.2$ channels is required *in vivo* for normal vascular regulation, cell-surface expression of $Ca_V1.2$ channels in cardiac myocytes, and $\beta$-adrenergic stimulation of L-type $Ca^{2+}$ currents in the heart.**

The $Ca_V1.2$ channel conducts L-type calcium ($Ca^{2+}$) current in cardiomyocytes, where $Ca^{2+}$ enters through the channel and initiates excitation-contraction coupling via $Ca^{2+}$-induced $Ca^{2+}$ release (1). Normal expression of $Ca_V1.2$ channels is required for cardiac contractile function and for survival beyond embryonic day 14 (2). Lack of the $Ca_V1.2$ channel also abolishes the development of myogenic tone and disrupts hormonal regulation of blood pressure (3). In contrast, deletion of $Ca_V1.3$, which also conducts L-type $Ca^{2+}$ currents, causes sinoatrial nodal dysfunction and cardiac arrhythmias but does not impair contractility or cause premature death (4). Overall, these gene deletion studies illustrate that L-type $Ca^{2+}$ currents are essential for normal cardiovascular function and for normal development.

$Ca_V1$ channels are multisubunit complexes composed of a pore-forming $\alpha1$ subunit and auxiliary $\beta$, $\alpha2\delta$, and in some cases $\gamma$ subunits (5–7). They are a primary target for regulation by numerous hormones, protein kinases, and phosphoprotein phosphatases (5–7). In the "fight-or-flight" response, increased force of contraction is achieved largely through regulation of $Ca_V1.2$ channels in the heart by the sympathetic nervous system through activation of $\beta$-adrenergic receptors, adenylyl cyclase, and cyclic AMP-dependent protein kinase (PKA) and resulting phosphorylation of $Ca_V1.2$ channels (1, 5, 6, 8). $\beta$-Adrenergic regulation of $Ca_V1.2$ channels requires A-kinase anchoring protein 15 (AKAP15),[2] which anchors the kinase to the distal C terminus of $Ca_V1.2$ via a modified leucine zipper (LZ) motif (9–11).

The C terminus of $Ca_V1$ channels undergoes proteolytic processing *in vivo* in skeletal and cardiac muscle (12–15). In cardiac muscle, the $\alpha1$ subunit of $Ca_V1.2$ channels is present in two size forms of ~240 and 210 kDa, which differ by truncation of the distal C terminus (DCT) (15). This truncation leads to enhanced activity of $Ca_V1.2$ channels expressed in *Xenopus* oocytes and mammalian cell lines (16, 17). Single channel conductance, modulation by $\beta$ and $\alpha2\delta$ subunits, and sensitivity to $Ca^{2+}$ channel agonists such as Bay K8644 remain unchanged (16, 17). The proteolytically cleaved DCT binds to the truncated channel and acts as potent autoinhibitor (18). Mutations of key charged residues at the interface between distal and proximal C-terminal domains of $Ca_V1.2$ relieves autoinhibition (18). Moreover, recent studies indicate that regulation of $Ca_V1.2$ channels can be reconstituted in transfected nonmuscle cells expressing a signaling complex of truncated $Ca_V1.2$, DCT, and AKAP15 (19).

To determine the regulatory roles of the DCT *in vivo*, we created a mouse line expressing only the truncated $Ca_V1.2$ channel ($Ca_V1.2\Delta DCT$) by introducing a premature stop codon at the site of proteolytic cleavage. Mice expressing only truncated $Ca_V1.2$ channels developed severe cardiac hypertrophy and died perinatally. Drugs that reduce peripheral vascular resistance improved survival, suggesting that premature death results from failure of vascular regulation. Cell-surface expression of $Ca_V1.2$ channels was dramatically reduced in myocytes from embryonic hearts but not in coronary vascular smooth

* This work was supported, in whole or in part, by National Institutes of Health Training Grants T32 GM07750 (to M. R. M.) and T32 NS07332 (to J. P. C.) and Research Grants P01 HL44948 and R01 HL85372 (to W. A. C.). This work was also supported by American Heart Association Postdoctoral Research Fellowship 10POST2630160 (to Y. F.).

[1] To whom correspondence should be addressed: Dept. of Pharmacology, Mailstop 357280, University of Washington, Seattle, WA 98195-7280. Tel.: 206-543-1925; Fax: 206-543-3382; E-mail: wcatt@uw.edu.

[2] The abbreviations used are: AKAP15, A-kinase anchoring protein 15; Het, heterozygous; DCT, distal C terminus.

muscle cells. Deletion of the DCT abolished regulation by PKA and reduced localized expression of AKAP15. Overall, our results reveal that the DCT of $Ca_V1.2$ channels is required for normal cardiovascular regulation, expression of $Ca_V1.2$ channels in cardiac myocytes, and regulation by β-adrenergic stimulation *in vivo*.

## EXPERIMENTAL PROCEDURES

The present study conformed to the guidelines for the Care and Use of Laboratory Animals of the National Institutes of Health and protocols approved by the Institutional Animal Care and Use Committee of the University of Washington. Animals were maintained under a standard 12:12-h light-dark cycle regime and had *ad libitum* access to standard chow and water except for specified drug treatments.

*Generation of $Ca_V1.2$ ΔDCT Mice*—A mouse line carrying a premature stop codon that results in the expression of the truncated channel was generated by Ingenious Targeting Laboratory (Stony Brook, NY). Approximately 11.5 kb of the *Cacna1c* gene containing exons 44 through 49 were isolated from a 129SvJ mouse genomic library. A targeting vector was constructed containing 1.1 kb of intronic sequence that extended from a site 0.3 kb upstream of exon 44 as its short arm followed by a 1.9-kb neomycin positive-selection cassette flanked by loxP sites and a 11.2-kb long arm that began at a site 0.3 kb upstream of exon 44 and extended to the NsiI site downstream of exon 49. To truncate the C terminus of $Ca_V1.2$ channels after G1796, a three-way stop codon cassette (5′-ctgagtaagta) was ligated into the NcoI site in exon 44 of the targeting construct. An NcoI-linearized targeting construct was transfected into 129Sv/Ev embryonic stem cells by electroporation. Clones were selected and expanded in the presence of G418. PCR analysis was used to identify clones that had undergone homologous recombination. The correctly targeted embryonic stem cell clones were microinjected into C57BL/6J blastocysts (The Jackson Laboratory, Bar Harbor, ME). Germ line transmission of the mutated *Cacna1c* allele was confirmed for one of three chimeric mice, and the resulting progeny were backcrossed into C57Bl/6J for more than 10 generations to generate heterozygous (Het) and homozygous $Ca_V1.2$ΔDCT (KO) animals used in this study.

*Genotyping*—Wild-type (WT) and mutant animals were identified by PCR analysis of tail-tip DNA using primers FH258 (CCCACTGCACATCAACAAGAC) and FH254 (GTCCTGTGTGGAAGACTCAAGGAG). The amplified product was further digested by NcoI, which gives a single band at 702 bp for the WT allele and at 908 bp for the mutated allele due to elimination of the NcoI restriction site in exon 44.

*Drug Treatments of $DCT^{-/-}$ Mice*—Heterozygotes ($DCT^{+/-}$, Het) were used to generate $DCT^{-/-}$ (KO) mice that only express $Ca_V1.2$ΔDCT. Pregnant Het female mice were sacrificed at gestational day 16–18. Embryos were removed by Cesarean section, and a tail sample was used for PCR analysis for genotyping. Due to the embryonic lethality of KO mice, a series of drugs were administered during the last week of gestation to prolong survival. Isradipine (1 or 3 mg/kg) and cyclosporin A (50 mg/kg) were administered via daily subcutaneous injections to pregnant female mice starting at E13. Tadalafil (0.5 μg/ml) and captopril (200 mg/liter) were given via drinking water from E13 to E18. Hearts were dissected and blotted dry for weight measurement to evaluate hypertrophy.

*Patency of Ductus Arteriosus*—Embryos at E18 were dissected after Cesarean section. The thoracic cavity was opened, and the atria were removed for better visualization of the ductus arteriosus. Ink was injected into the right ventricle and visualized under a dissection microscope.

*Isolation and Culture of Embryonic Cardiomyocytes*—Embryonic cardiomyocytes were isolated similarly to Davies *et al.* (20). Atria were separated from the heart. The ventricles were cut into small pieces with a razor blade and transferred to ADS buffer containing 5 mM NaCl, 20 mM HEPES, 1 mM $NaH_2PO_4$, 5.5 mM glucose, 5 mM KCl, 0.8 mM $MgSO_4$ (pH 7.35). After a short centrifugation, the buffer was replaced with ADS containing 0.5 mg/ml Collagenase II (Worthington Biochemical). The tissue blocks were digested for two 20-min cycles at 37 °C on a rotating plate followed by gentle trituration. After a quick centrifugation, the supernatant was transferred to a tissue culture dish or plated on laminin-treated glass coverslips. Cells were cultured in 37 °C in DMEM with 10% fetal bovine serum and used within 48 h after isolation for electrophysiological measurements.

*Histology and Immunocytochemistry*—Embryos were fixed in 4% paraformaldehyde and cryoprotected by sinking in 30% (w/v) sucrose in 0.1 M sodium phosphate at 4 °C for 72 h. Tissues were cut into 80-μm coronal sections and mounted on subbed slides for hematoxylin and eosin staining and immunocytochemistry. As described previously (21), tissues slices and myocytes were permeabilized by 0.025% Triton X-100 after fixation and probed with corresponding antibodies. Mouse monoclonal antibody ($Ca_V1.2$m, clone L57/46) against the proximal C terminus of $Ca_V1.2$ channels was purchased from UC Davis/NIH NeuroMab Facility. Polyclonal anti-$Ca_V1.2$ (anti-CNC1) and anti-$Ca_V1.3$ (anti-CND1) were generated against amino acid sequences in the intracellular loop betweens domains II and III of $Ca_V1.2$ and $Ca_V1.3$ channels (22) and characterized previously (9, 23). Monoclonal antibody against RyR2 was purchased from Millipore Corp. The DCT was immunostained using anti-CH1 that specifically recognizes the DCT of $Ca_V1.2$ (15, 24). A specific anti-peptide antibody against AKAP15 was prepared as previously described (25).

*Electrophysiology*—The whole-cell configuration of the patch clamp technique was used to record $Ca^{2+}$ currents from embryonic ventricular myocytes isolated at E16-E18. Currents were recorded with an Axopatch 200B amplifier (Molecular Devices, Sunnyvale, CA). Data acquisition and command potentials were controlled by Pulse software (Heka Electronics), and data were stored for later analysis with IGOR (Wavemetrics, Lake Oswego, OR). Residual leak and capacitive transients were subtracted using a P/4 protocol. The extracellular bath solution contained 140 mM tetraethylammonium chloride, 2 mM $MgCl_2$, 20 mM $BaCl_2$, 10 mM Hepes, and 10 mM glucose (pH 7.4). The intracellular solution contained 100 mM CsCl, 20 mM tetraethylammonium chloride, 1 mM $MgCl_2$, 5 mM MgATP, 10 mM Hepes, and 10 mM EGTA (pH 7.3). Control and forskolin-containing medium was rapidly perfused from a gravity-fed system. Cells were held at −40 mV to inac-

tivate T-type $Ca^{2+}$ channels and $Na^+$ channels, and 100-ms test pulses were applied from −40 to +40 mV in 10-mV increments. Peak $Ba^{2+}$ current amplitude was plotted *versus* voltage to generate current-voltage (I-V) relationships. To measure the voltage dependence of activation, tail currents were recorded after repolarization to −50 mV after test pulses from the holding potential to potentials from −50 to +150 mV in 10-mV increments. To measure inactivation kinetics, $Ba^{2+}$ current was recorded after a series of 1-s depolarizations from the holding potential of −40 mV to potentials from 0 to +30 mV in 10-mV increments. The results were normalized to peak $Ba^{2+}$ current amplitude recorded at +10 mV. For analysis of inactivation kinetics, individual data traces were smoothed using a binomial algorithm with an interval of 20 points. Gating-charge movement was measured by applying a series of test pulses at 10-s intervals from a holding potential of −40 mV to potentials between +60 to +80 mV in 2-mV increments and integrating the gating charge movement at the reversal potential for the ionic currents (18). Patch pipettes (2–4 megaohms) were pulled from micropipette glass and fire-polished before use. Recordings were discarded if the series resistance was >7 megaohms before compensation. All experiments were performed at room temperature.

*Quantification of Immunocytochemical Images*—For analysis of fluorescence intensity of $Ca_V1.2$ channels and AKAP15, whole regions of interest were taken from the images, and mean pixel intensities were determined.

*RT-PCR*—Total RNA was extracted from whole hearts of WT, Het, and KO embryos. $Ca_V1.2$ mRNA expression was analyzed by RT-PCR using fluorescent SYBR Green technology on a StepOnePlus system (Applied Biosystems). Standard curves were constructed from cDNA standards, and the results were normalized by expression as a molar ratio to acidic ribosomal protein.

*Statistics and Significance*—All of the data are reported as the means ± S.E. One-way ANOVA with a Bonferroni posttest (GraphPad Prism 4.0) was used to compare the averages from multiple groups.

## RESULTS

*Genotype*—A mouse line expressing the truncated $Ca_V1.2$ channel was generated by introducing a premature stop codon at G1796 (Fig. 1*A*). Genotype was determined by loss of a NcoI restriction site (Fig. 1, *B–D*). Germ line transmission was confirmed using RT-PCR with different primer pairs (Fig. 1*E*). When probed with an anti-$Ca_V1.2$ antibody that recognizes an epitope in the intracellular loop connecting domains II and III, sections from hearts of E16 WT and KO mice had easily detectable levels of $Ca_V1.2$ channels (Fig. 1*F*). In contrast, no signal was detected using an antibody against the truncated distal C terminus in $DCT^{-/-}$ heart, confirming successful deletion of the DCT. Two unexpected splice variants with short extensions of 3 and 12 residues beyond G1796 were identified (Fig. 1*D*). mRNA encoding the truncated $Ca_V1.2$ channel with the 12-amino acid extension was most abundant. However, this 12-residue extension has no effect on expression and function of the truncated $Ca_V1.2$ channel in transfected tsA-201 embryonic kidney cells (Fig. 1, *G* and *H*).

*Premature Death of $DCT^{-/-}$ Mice*—Heterozygous $Ca_V1.2\Delta DCT$ mice containing one truncated allele show no distinguishable phenotypic differences from WT littermates, whereas no homozygous mice were found at weaning. Further analysis revealed that $DCT^{-/-}$ mice died shortly after birth, usually within a few hours. No survival was observed after 24 h. To determine the timeline of death of $DCT^{-/-}$ mice, we examined the genotype distribution during embryonic development from E13 to E18. Live $DCT^{-/-}$ embryos were found at a lower than expected Mendelian ratio (Fig. 2*A*, $p < 0.01$). Death of $DCT^{-/-}$ embryos occurred as early as E15 and throughout the later gestational stage until birth. These results indicate that regulation of the $Ca_V1.2$ channel by its DCT is required for normal embryonic development *in vivo*.

*Cardiac Hypertrophy and Heart Failure in $DCT^{-/-}$ Mice*—Significant abdominal blood pooling was observed in all dead $DCT^{-/-}$ embryos and pups collected after birth (Fig. 2*A*), a hallmark feature of congestive heart failure. No other difference in gross structure or morphology was observed between WT and $DCT^{-/-}$ embryos. $DCT^{-/-}$ embryos had an ~31% increase in heart weight to body weight ratio compared with WT (Fig. 2*C*, 5.5 ± 0.2 *versus* 4.2 ± 0.1 mg/g, $p < 0.001$), indicating severe cardiac hypertrophy. Unlike the left ventricular hypertrophy observed in humans and animal models of heart failure, the hypertrophy in $DCT^{-/-}$ embryos occurs preferentially in the right ventricle as shown in Fig. *2B*. Enlarged hearts were observed in all dead $DCT^{-/-}$ embryos and pups. Further histological analysis with hematoxylin and eosin staining demonstrated significant concentric hypertrophy in the right ventricular chamber (Fig. 2*B*), which would limit the diastolic volume and thereby impair contractile function and pumping capacity. Therefore, the right ventricular hypertrophy we have observed may cause impaired pumping capacity and pooling of blood in internal organs such as the gastrointestinal track and liver, contributing to heart failure and death of $DCT^{-/-}$ mice.

Membrane capacitance is proportional to cell surface area, providing a quantitative estimate of cell size. Dissociated myocytes from $DCT^{-/-}$ mice have a shift in distribution of cell-surface area, with fewer myocytes having single-cell capacitances of 20–25 picofarads and more myocytes having capacitances of 30–35 picofarads (Fig. 2*D*). Hypertrophied myocytes often appeared larger in cell culture and typically expressed lower levels of $Ca_V1.2$ channels in cytoplasm and plasma membrane in immunocytochemical images (Fig. 2*E*). Overall, these results indicate that truncation of $Ca_V1.2$ channels leads to hypertrophy of individual cardiac myocytes, which increases the size and impairs the function of the right ventricle.

*Rescue of $DCT^{-/-}$ Embryos with Vasodilator Treatment*—The preferential hypertrophy of right ventricle prompted us to investigate whether the ductus arteriosus remains patent in $DCT^{-/-}$ embryos. The ductus arteriosus is a specialized vascular structure for fetal circulation that connects the pulmonary trunk to the descending aorta and allows shunting of 95% of the blood away from the high resistance pulmonary vasculature. Because of this shunt, the right ventricle plays a much more important role in pumping blood to the peripheral circulation compared with adult heart. Premature clo-

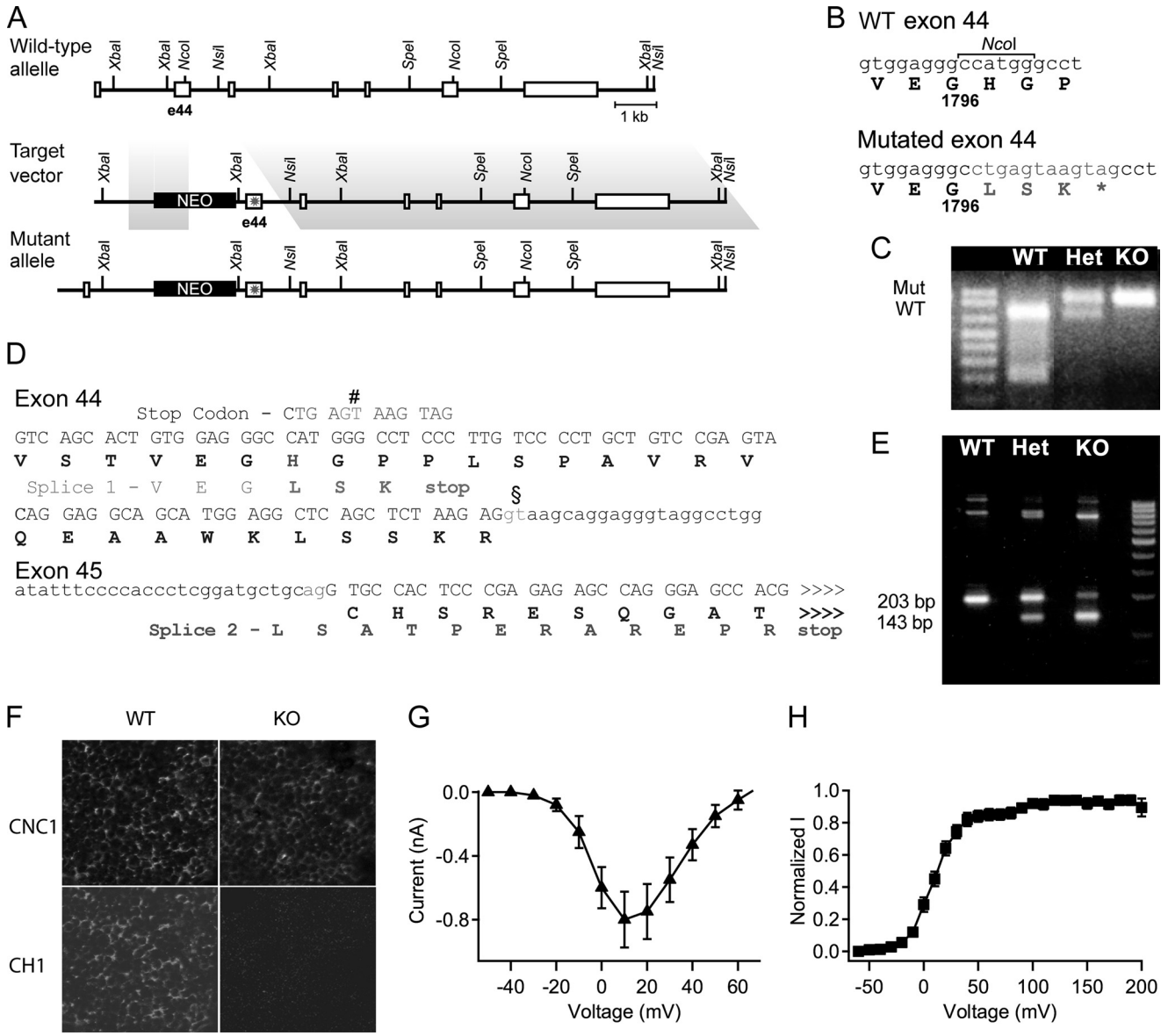


FIGURE 1. **Generation of $Ca_V1.2\Delta DCT$ mice.** *A*, a diagram of the targeting strategy used to generate $Ca_V1.2\Delta DCT$ mice by homologous recombination to truncate the $Ca_V1.2$ channel. Homologous recombination of the targeting construct with the *Cacna1c* gene resulted in a mutated allele in which a three-way stop codon cassette was inserted. The targeting vector consists of a short arm of 1.1 kb followed by neomycin (*NEO*) cassette flanked by loxP sites and an 11.2-kb long-arm that began at a site 0.3 kb upstream of exon 44 bound by a NsiI site downstream of exon 49. A three-way stop codon cassette (5′-ctgagtaagtag) was ligated into a blunted NcoI site in exon 44 of the targeting construct to engineer a premature stop. Homologous recombination leads to incorporation of Neo selection cassette and premature stop codon into genomic DNA of the *Cacna1c* gene. *B*, partial amplicons obtained by the primer pair used for genotyping were sequenced and aligned with the cDNA and amino acid sequence of $Ca_V1.2$. *Lowercase letters*, sequence of exon 44 for wild-type and mutant; *second line*, amino acid sequence of wild-type and mutant protein. *, premature stop codon downstream of the three-way stop codon cassette. *C*, PCR amplification products from genomic DNAs of WT, Het ($DCT^{+/-}$), and KO ($DCT^{-/-}$) embryos were subjected to NcoI digestion. An NcoI site is present in the WT but not the mutant construct. A 702-bp product is obtained for the WT allele, whereas the uncut mutant allele is 908 bp. *D*, DNA sequence analyses of the RT-PCR products from mRNAs encoding the C terminus of $Ca_V1.2\Delta DCT$. The expected ~210-bp RT-PCR product encodes the expected C-terminal sequence ending at Gly-1796 with an extension of Leu-Ser-Lys-stop (*bold*). However, there is also an unexpected alternative RNA splicing variant due to a splice donor site (§) in Exon 44 and a splice acceptor site in Exon 45. Splicing via the alternative splice donor site (#) produces a +1 nucleotide shift of the Exon 45 reading frame, and a 12-amino acid-residue peptide extension (LSATPERAREPR) after Gly-1796 in the truncated C terminus of $Ca_V1.2$ channels. *E*, RT-PCR of brain mRNA from WT and mutant $Ca_V1.2\Delta DCT$ mice is shown. Multiple sets of oligonucleotides were used to amplify mRNA splice products spanning the exons 44 and 45 splice junction. The alternative splice variant gives rise to a ~143-bp RT-PCR product instead of the predicted ~210 bp for mutant allele. The ratio of RT-PCR products indicates that the 143-bp splice product accounts for the majority of the mRNA. *F*, coronal heart sections from WT and KO mice at E16 were analyzed by immunocytochemistry. *Top*, anti-CNC1 recognizes the intracellular loop between domains I and II of $Ca_V1.2$ channels. *Bottom*, anti-CH1 recognizing the distal C-terminal tail of $Ca_V1.2$ ($Ca_V1.2DCT$). *Scale bar* = 25 $\mu$m. *G*, I-V relationship. *H*, voltage dependence of activation. These parameters were unchanged relative to unextended $Ca_V1.2$ ΔDCT channels (not shown) expressed in tsA-201 cells.

sure of the ductus arteriosus results in cardiac hypertrophy and right-sided heart failure (26). We examined live $DCT^{-/-}$ embryos, all of which show enlarged right ventricles but no closure of the ductus arteriosus (Fig. 3*A*). These results rule out anatomical closure of the ductus arteriosus as the cause of hypertrophy in $DCT^{-/-}$ mice, but it remains possible that increased contracture of the ductus arteriosus could contribute to right ventricular hypertrophy in $DCT^{-/-}$ mice.

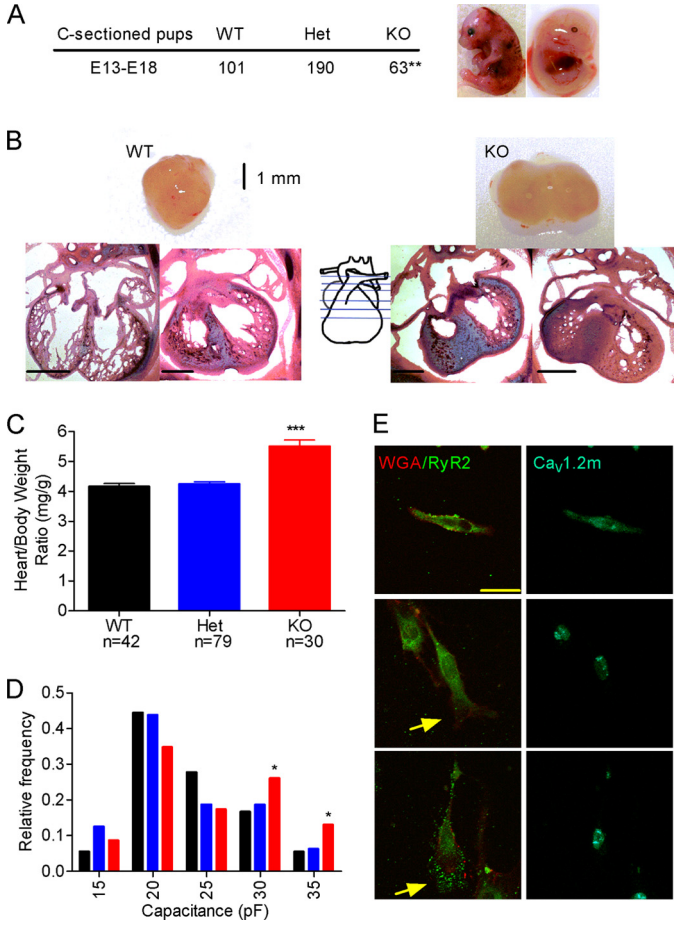


FIGURE 2. **Phenotypes of $Ca_V1.2\Delta DCT$ mice.** *A*, $Ca_V1.2\Delta DCT$ KO mice have reduced survival rates during embryonic development from E13 to E19 as indicated by the sub-Mendelian numbers of KO animals. Deaths occur as early as E15, but some embryos survive until hours after birth. *Right panel*, examples of KO embryos show marked abdominal blood pooling. *B*, cardiac hypertrophy of KO mice. *Top*, examples of WT and KO hearts. *Bottom*, coronal sections of WT (*left*) and KO (*right*) hematoxylin and eosin-stained hearts. *Scale bar* = 1 mm. *C*, ratio of heart weight to body weight is shown. *D*, a histogram of distribution of cell capacitances for cells isolated from animals of each genotype (*colors* correspond to genotype as in *panel C*). *E*, cells isolated from WT hearts (*upper panel*) and KO hearts (*lower panel*) stained with wheat germ agglutinin labeled with Alexa 555 as a cell membrane marker (*red*) (*anti-WGA*), anti-RyR2 (*green*), or anti-$Ca_V1.2$. KO cells were hypertrophied with blebbing and extension of membrane at the end of the cell (*arrows in lower two panels*) compared with WT Cells (*upper panel*). *Scale bar* = 10 $\mu$m.

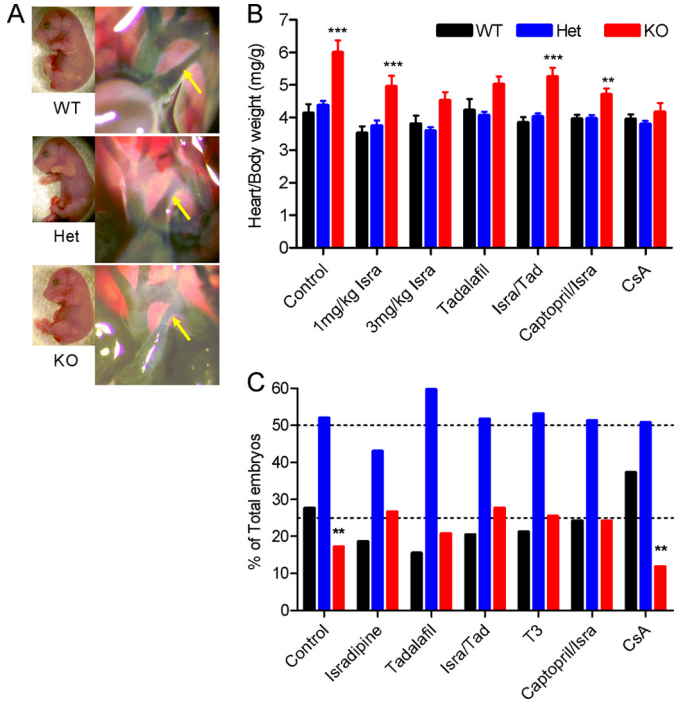


FIGURE 3. **Role of ductus arteriosus and peripheral vascular resistance in producing hypertrophy.** *A*, images of the ink-filled ductus arteriosus (*arrows*) in hearts from animals of each genotype. No gross abnormalities were detected in the vascular structure of KO mice. *B* and *C*, cardiac hypertrophy (*B*) and embryonic survival (*C*) were evaluated after the indicated drug treatments from E13 to E18. For each drug or drug combination, at least five litters of animals were tested. Significant differences in hypertrophy and survival are indicated by *asterisks*. *Isra*, isradipine; *CsA*, cyclosporin; *Tad*, tadalafil.

Based on our *in vitro* data (18), we expected that truncation of the DCT would lead to up-regulation of $Ca_V1.2$ channel activity in cardiac and vascular smooth muscle cells, and this increased activity could lead to increased peripheral vascular resistance, hypertension, and heart failure. Human hypertension is treated with dihydropyridine calcium channel blockers, which preferentially inhibit $Ca_V1.2$ channels in vascular smooth muscle cells *in vivo* (27, 28). The calcium channel antagonist isradipine (1 and 3 mg/kg) reduced the heart to body weight ratio significantly and increased survival of $DCT^{-/-}$ embryos assayed at E18 (Fig. 3, *B* and *C*). This effect was dose-dependent, but no further improvement was observed at 10 mg/kg. This result suggests the possibility that overactive $Ca^{2+}$ channels in vascular smooth muscle are responsible for hypertrophy and premature death in $DCT^{-/-}$ mice.

Angiotensin-converting enzyme inhibitors are the most widely used treatment for human hypertension. We found that captopril plus isradipine did not substantially improve heart weight or survival compared with isradipine alone (Fig. 3, *B* and *C*). The specific cyclic nucleotide phosphodiesterase-5 (PDE5) inhibitor tadalafil is an effective treatment for pulmonary hypertension in humans, and it has also been shown to inhibit PDE5 in ductus arteriosus and cause dilation of the shunt in the fetus (29). Tadalafil was approximately as effective as isradipine in reducing heart weight and premature death when given alone, but the combined effects of tadalafil and isradipine were not greater than isradipine alone (Fig. 3, *B* and *C*).

These results suggested that increased vascular resistance due to overactive $Ca^{2+}$ channels contributes significantly to the development of cardiac hypertrophy and thereby to premature death of $DCT^{-/-}$ animals during embryonic development. To test whether the cardiac hypertrophy *per se* results in the death of $DCT^{-/-}$ embryos, we used the calcineurin inhibitor cyclosporin A, which counteracts the effects of alterations in $Ca^{2+}$ signaling and effectively protects the heart from cardiac hypertrophy (30–33). Treatment with cyclosporin A almost completely prevented hypertrophy in $DCT^{-/-}$ embryos (Fig. 3*B*). Surprisingly, however, the survival ratio of $DCT^{-/-}$ embryos did not change (Fig. 3*C*). These results suggest that cardiac hypertrophy *per se* is not the primary cause of premature death of $DCT^{-/-}$ embryos and point to increased contracture of vascular smooth muscle in resistance vessels and resulting hypertension as a primary cardiovascular defect that causes premature death in $DCT^{-/-}$ mice.

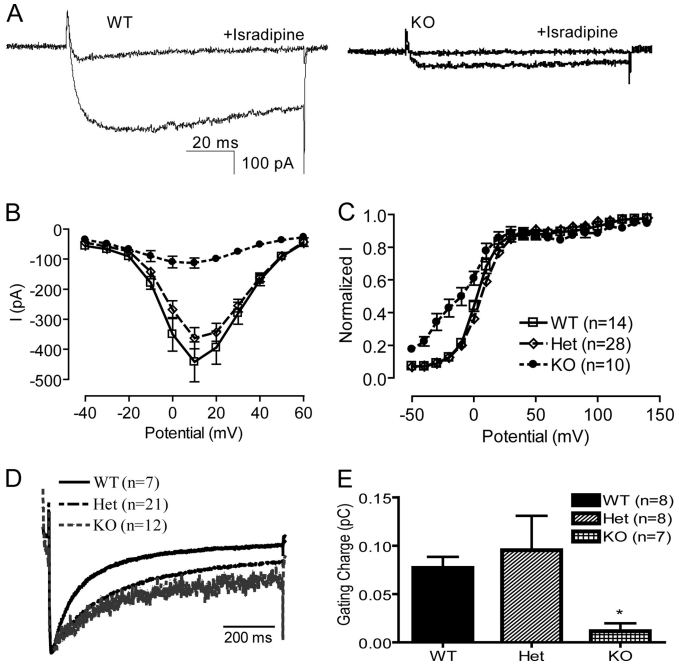


FIGURE 4. **Function and modulation of $Ba^{2+}$ currents through L-type channels.** *A*, $Ba^{2+}$ current from myocytes isolated from WT (*left*) and KO (*right*) animals in control and in the presence of 10 $\mu$M isradipine. *B*, mean I-V relationships for cells of each phenotype derived from peak currents during depolarizations to the indicated potentials. *C*, activation curves for L-type $Ba^{2+}$ currents derived from tail currents recorded at −50 mV after depolarizations to the indicated potentials and normalized to the largest tail current in each series of test pulses. *D*, mean currents recorded from cells of each genotype during 1-s depolarizations from −40 to +10 mV. *E*, mean gating charge measured at the reversal potential for cells of each genotype. *pC*, pico coulomb.

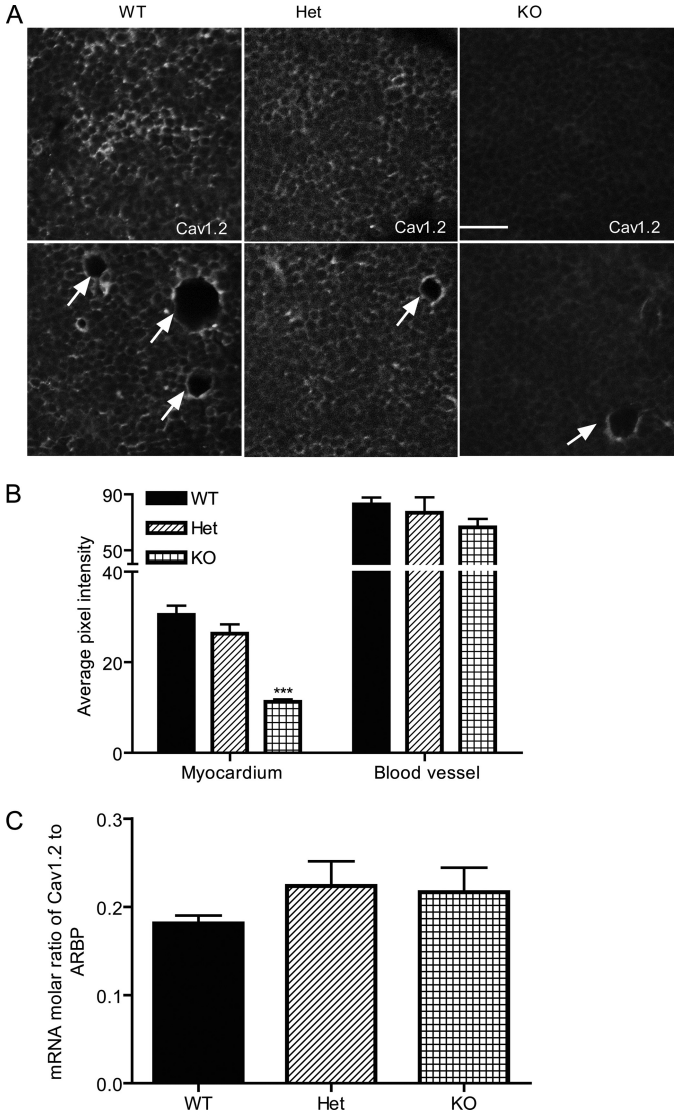


FIGURE 5. **Reduced expression of $Ca_V1.2$ channels in KO hearts but not blood vessels.** *A*, representative ventricular tissue slices from WT, Het, and KO E18 hearts stained with antibody recognizing the proximal C terminus of $Ca_V1.2$. Representative blood vessels (*arrows*) are shown in the *lower panel*. *B*, mean pixel intensity for $Ca_V1.2$ staining of WT, Het, and KO in myocytes *versus* blood vessels. *C*, mRNA levels of $Ca_V1.2$ expressed as a molar/molar ratio to acidic ribosomal protein (*ARBP*). *Scale bar* = 25 $\mu$m.

Even though treatment with isradipine, captopril, and tadalafil improved the survival of $DCT^{-/-}$ embryos to E18, none of them increased the number of pups surviving to weaning. The combination of captopril and isradipine was the most effective treatment, supporting survival to postnatal day 4 for a small fraction of $DCT^{-/-}$ pups. All other treatments failed to improve postnatal survival beyond 24 h.

*Reduced L-type $Ca^{2+}$ Current and $Ca_V1.2$ Expression in $DCT^{-/-}$ Hearts*—Using the whole-cell voltage clamp technique, we examined L-type $Ca^{2+}$ current in acutely dissociated embryonic cardiomyocytes. Current amplitude in WT myocytes is very small, even with 3.6 mM extracellular Ca. Therefore, 20 mM $Ba^{2+}$ was used as the charge carrier to achieve a better signal-to-noise ratio. L-type $Ba^{2+}$ current amplitude (Fig. 4, *A* and *B*) is dramatically reduced in cells of $DCT^{-/-}$ mice compared with those of WT and Het. At a holding potential of −40 mV, which inactivates $Na^+$ current and T-type $Ca^{2+}$ current, 10 $\mu$M isradipine completely blocked $Ba^{2+}$ current in both WT and $DCT^{-/-}$ cells, indicating that the dihydropyridine-sensitive L-type $Ca^{2+}$ current is selectively recorded under these conditions. The reduced L-type current in $DCT^{-/-}$ myocytes is surprising because truncated $Ca_V1.2$ channels expressed in non-muscle cells *in vitro* exhibit enhanced activity (17, 18).

Measurements of gating charge movement provide an estimate of the number of functional voltage-gated ion channels on the cell surface whose voltage sensors can be activated by depolarization (34). Most of the rapid gating charge movement in single dissociated cardiac myocytes upon depolarization from a holding potential of −40 mV reflects activation of $Ca_V1.2$ channels (35, 36). The gating charge movement measured at the reversal potential was significantly lower in $DCT^{-/-}$ cells compared with WT (Fig. 4*E*). This suggests that the surface expression of truncated $Ca_V1.2$ channels is dramatically reduced, which explains the lower peak current amplitude in these cells.

We used immunocytochemistry with specific antibodies to further assess the expression of $Ca_V1.2$ channels in $DCT^{-/-}$ myocytes and vascular smooth muscle cells. In both acutely dissociated cardiomyocytes (not shown) and transverse sections of heart from $DCT^{-/-}$ mice, specific immunostaining of $Ca_V1.2$ channel was greatly reduced (Fig. 5). On the other hand, the expression of other proteins that are involved in $Ca^{2+}$ signaling in cardiomyocytes such as ryanodine receptor and

$Ca_V1.3$ channels remained unchanged (data not shown). These results confirm that expression of $Ca_V1.2$ channels in cardiac myocytes is impaired by deletion of the DCT. In contrast, specific immunostaining of $Ca_V1.2$ channel in blood vessels (indicated by *arrows*) remained unchanged (Fig. 5, *A*, *lower panels*, and *B*). The level of mRNA encoding $Ca_V1.2$ channels in the heart remains the same for all three genotypes (Fig. 5*C*), suggesting that deletion of the DCT impairs the protein assembly and/or lifetime at the plasma membrane of cardiomyocytes rather than gene expression. The reduced expression of $Ca_V1.2$ channels in cardiac myocytes, but not in vascular smooth muscle, may create an imbalance in the cardiovascular system in which cardiac output is compromised by reduced $Ca_V1.2$ channel expression in cardiac myocytes at the same time as peripheral vascular resistance is increased by deletion of the DCT and increased activity of the normal number of $Ca_V1.2$ channels in vascular smooth muscle.

*Activation and Inactivation of $Ca_V1.2\Delta DCT$*—In addition to the large reduction in peak L-type $Ba^{2+}$ current, we also observed a substantial negative shift in voltage dependence of activation of $Ca_V1.2\Delta DCT$ channels (Fig. 4*C*). However, the precise extent of this negative shift should be viewed with caution considering the small current amplitude in $DCT^{-/-}$ cells. In addition to the negative shift in the voltage dependence of activation, voltage-dependent inactivation of the L-type $Ba^{2+}$ current conducted by $Ca_V1.2\Delta DCT$ channels was significantly slowed (Fig. 4*D*). Interestingly, voltage-dependent inactivation was also slowed in Het cells, where the current amplitude and voltage dependence of channel activation remained indistinguishable from WT, suggesting that the rate of inactivation may be preferentially affected by the loss of DCT. This result is consistent with our recent studies showing that the DCT is required for the normal enhancement of voltage-dependent inactivation of $Ca_V1.2$ channels by physiological levels of intracellular $Mg^{2+}$ (37).

*Regulation of $Ca_V1.2\Delta DCT$ Channels by the β-Adrenergic/PKA Pathway*—Upon β-adrenergic activation of cardiac myocytes, PKA phosphorylates $\alpha_1$ and β subunits of the $Ca_V1.2$ channel (15, 23, 38, 39), which increases peak $Ca^{2+}$ currents, increases the maximal probability of channel opening and negatively shifts the voltage dependence of channel activation (6, 8, 40). The β-adrenergic receptor agonist isoproterenol increases $Ca^{2+}$ current of embryonic cardiomyocytes isolated at E16-E18 by ~2-fold and shifts the voltage dependence of activation to more negative membrane potential (data not shown), indicating that the fetal cardiomyocyte is a valid system to examine the regulation of β-adrenergic signaling pathway. However, this response is heavily dependent on the maturation of cells because robust coupling of β-adrenergic receptors to G proteins is not fully established until birth (41). Therefore, we chose to activate adenylyl cyclase directly, downstream of β-adrenergic receptors and G proteins, using forskolin. Extracellular perfusion of 10 μM forskolin increased the current amplitude in both Het and WT cells by ~2-fold (Fig. 6). In contrast, no enhancement of $Ba^{2+}$ current was observed in $DCT^{-/-}$ cells. This result suggests that the DCT is a critical regulatory element that is required for regulation by the β-adrenergic/PKA pathway *in vivo*. It is also consistent with other studies

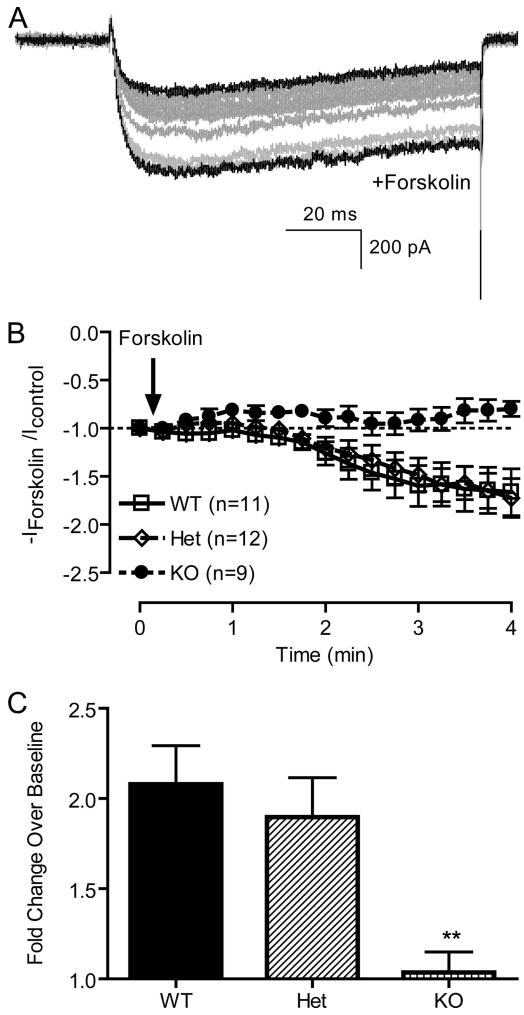


FIGURE 6. **Forskolin regulation of $Ba^{2+}$ current in cardiac myocytes.** *A*, $Ba^{2+}$ current elicited by depolarization from −40 to +10 mV was measured during extracellular perfusion with control solution or solution containing 10 μM forskolin. Traces recorded every 15 s from a representative cell are shown. *B*, peak current amplitude was derived from each depolarization and normalized to base-line current amplitude. -Fold change over base line was plotted. *C*, maximal response to forskolin in each cell was normalized to base-line $Ba^{2+}$ current, and the means of -fold change for cells of each genotype are shown.

showing that the full-length $\alpha_{1C}$ subunit but not the truncated form is phosphorylated in response to elevated cAMP *in vitro* (15, 42–45). Our results provide the first demonstration *in vivo* that the truncated $Ca_V1.2$ channel alone, without the proteolytically processed DCT, is not sufficient for up-regulation by β-adrenergic stimulation.

*Association of AKAP15 with $Ca_V1.2\Delta DCT$ Channels*—AKAP15 has been demonstrated to anchor PKA to $Ca_V1.2$ channels in heart through interaction with the AKAP binding domain located in the DCT (9). This interaction is required for effective regulation by PKA even though the AKAP binding domain is located beyond the point of proteolytic truncation of the DCT (9). To assess the importance of the DCT in localization of AKAP15 *in vivo*, we measured its expression and localization by immunocytochemistry with specific antibodies. We found that the specific staining of AKAP15 is reduced in cardiac cells dissociated from $DCT^{-/-}$ animals (data not shown). A similar reduction in immunostaining was also observed in transverse sections from

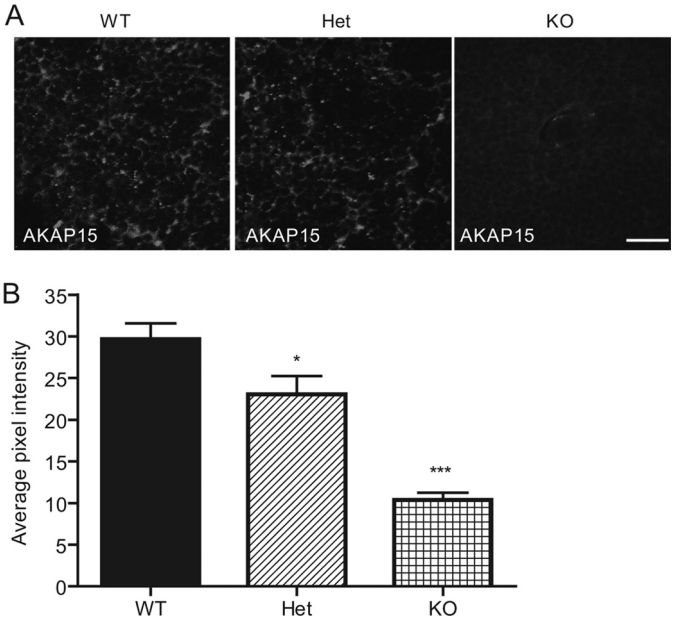


FIGURE 7. **Expression of AKAP15 in WT, Het, and KO hearts.** *A*, representative ventricular tissue sections from WT, Het, and KO E18 hearts stained with antibody recognizing AKAP15. *B*, mean pixel intensity of AKAP15 in ventricular slices. *Scale bar* = 25 $\mu$m.

heart tissue (Fig. 7). These results indicate that the DCT of $Ca_V1.2$ channels is required for normal expression and localization of AKAP15 in cardiac myocytes.

## DISCUSSION

*Functional Roles of the DCT of $Ca_V1.2$ Channels in Vivo*—Our studies of mice with deletion of the DCT of $Ca_V1.2$ channels have shown that this regulatory domain is required for life and has at least three essential functions. First, we find that deletion of the DCT induces cardiac hypertrophy and failure, possibly as a result of impairment of regulation of the peripheral vasculature. These results demonstrate an essential role for the DCT in cardiovascular regulation *in vivo*. Second, against expectations from *in vitro* expression studies, we find that deletion of the DCT reduced the function and cell-surface localization of $Ca_V1.2$ channels, demonstrating a requirement of the DCT for normal functional channel expression in cardiac myocytes. Third, our results show that $Ca_V1.2\Delta$DCT channels cannot be regulated by the $\beta$-adrenergic/PKA signaling pathway and cannot support normal expression and localization of AKAP15. Each of these functional effects of the DCT is considered in more detail below.

*Deletion of the DCT of $Ca_V1.2$ Channels Causes Right Ventricular Hypertrophy and Heart Failure*—Increased peripheral vascular resistance leads to hypertension and heart failure (46). Hypertension in humans is effectively treated with the calcium channel blocker isradipine and the angiotensin-converting enzyme inhibitor captopril (27, 28, 47). In addition, pulmonary hypertension in humans is effectively treated with tadalafil (48). Our experiments show that deletion of the DCT of $Ca_V1.2$ channels in mice causes dramatic right ventricular hypertrophy and heart failure that are improved, but not cured, by treatment with isradipine, captopril, tadalafil, and combinations of those drugs. These results demonstrate a requirement for the DCT of $Ca_V1.2$ channels in normal regulation of the cardiovascular system *in vivo*.

$Ca_V1.2$ knock-out mice die before embryonic day 14, and their death was proposed to be caused by lack of functional $Ca_V1.2$ channels in the heart (2). This hypothesis was confirmed by the generation of viable conditional knock-out animals with $Ca_V1.2$ channels inactivated in vascular smooth muscle cells (3), in insulin-secreting cells in the pancreas (49), or in the hippocampus and neocortex of the brain (50). These studies show that loss of function of $Ca_V1.2$ channels in vascular smooth muscle is not lethal, whereas loss of function in cardiac myocytes leads to premature death before E14. In light of these previous results, it is most likely that the failure of cardiovascular function in $Ca_V1.2\Delta$DCT mice is caused by the combination of gain-of-function of the normal number of $Ca_V1.2$ channels in vascular smooth muscle cells with loss of expression in cardiac myocytes. Together, these two effects would create an imbalance between increased peripheral vascular resistance and decreased ventricular contractility, eventually leading to heart failure and premature death.

Unfortunately, the small size of E16–18 embryos precludes detailed studies of the function of the cardiovascular system to determine the source of failure of cardiovascular regulation precisely. However, $Ca_V1.2$ channels have been suggested to act as $Ca^{2+}$ sensors for depolarization-induced $Ca^{2+}$ release in vascular smooth muscle (51), thereby playing an important role in maintaining myogenic tone and peripheral resistance. $Ca_V1.2$ channels also mediate blood pressure regulation by various hormones, such as angiotensin II (3). Therefore, it is expected that up-regulation of $Ca_V1.2$ channel activity in vascular smooth muscle cells would lead to increased vascular resistance and pressure overload to the heart. Our results show that $Ca_V1.2$ channels are expressed at normal levels in the coronary vasculature, in contrast to the loss of expression in cardiac myocytes, and it is expected that these channels in the vasculature would be hyperactive because of loss of the autoinhibitory DCT. Future studies of regulation of contractility and $Ca^{2+}$ channel function in dissociated vascular smooth muscle cells from $Ca_V1.2\Delta$DCT mice may provide further information on the source of impaired cardiovascular regulation.

*Differential Effects of DCT Truncation of Cardiac $Ca_V1.2$ Channels in Vitro and in Vivo*—Using *in vitro* heterologous expression systems, several groups have shown that removal of as many as 478 amino acids from distal C terminus of $Ca_V1.2$ increases current density, gating charge movement, and channel opening without affecting cell surface expression (16–18). Although the proteinase responsible for the proteolytic processing of $Ca_V1.2$ channels *in vivo* remains unknown, introduction of trypsin or carboxypeptidase A into cardiomyocytes results in an enhancement in L-type $Ca^{2+}$ currents (52, 53). Therefore, we expected that cardiac myocytes expressing only truncated $Ca_V1.2$ channels would have enhanced channel activity. In contrast to these expectations, however, the L-type $Ca^{2+}$ current measured in dissociated cardiomyocytes is dramatically reduced as a consequence of reduced cell-surface expression of the truncated channels. The drastic down-regulation of $Ca_V1.2$ channels in cardiac myocytes observed in our model is not characteristic of heart failure in general. Although

the alteration in $Ca_V1.2$ channel expression in hypertrophied and failing hearts remains controversial and inconclusive, no drastic up- or down-regulation was observed in most studies (54–57). Therefore, down-regulation of $Ca_V1.2$ channel expression is more likely to be a direct consequence of deletion of the DCT rather than a secondary consequence of heart failure. Deletion of the DCT would impair *in vivo* proteolytic processing at the point of truncation, which may be required for normal functional expression and cell-surface localization in cardiac myocytes. It is also possible that deletion of the DCT may result in failure of regulation in $Ca_V1.2$ gene expression, as the DCT has been shown to act as a transcriptional regulator (58) and to autoregulate $Ca_V1.2$ promoter activity *in vivo* in cardiac myocytes (59). However, we found no effect of deletion of the DCT on the level of mRNA encoding $Ca_V1.2$ channels in the heart. Therefore, it is most likely that the loss of expression of $Ca_V1.2$ channels in $DCT^{-/-}$ mice is caused by failure of proteolytic processing and assembly of the channel complex at the cell surface or by enhanced internalization from the cell surface and degradation.

*The DCT of $Ca_V1.2$ Channels Is Required for β-Adrenergic/PKA Regulation in Cardiomyocytes in Vivo*—Stimulation of cardiac L-type $Ca^{2+}$ current by epinephrine was first described in 1966 and hypothesized to be mediated by phosphorylation by PKA (8, 60–62). The increase in $Ca^{2+}$ currents observed after activation of PKA is due to an increase in the open-state probability of the channel resulting from a shift in gating mode (5, 42). Regulation of $Ca_V1.2$ channel requires PKA anchored to the DCT by AKAP15 or another AKAP (9, 10, 18, 19, 43), and the DCT is required for regulation of $Ca_V1.2$ channels in virally infected cardiac myocytes (63). The full-length $\alpha_{1C}$ subunit is phosphorylated both *in vitro* and *in vivo* by PKA in response to elevated cAMP, whereas the truncated $Ca_V1.2$ channel is not (15, 42–45). Multiple potential PKA phosphorylation sites in $\alpha_{1C}$ subunit have been identified (64). Phosphorylation of serine 1928 in the DCT is observed upon β-adrenergic stimulation and PKA activation in transfected cells and in cardiac myocytes; however, the functional impact of phosphorylation of serine 1928 *in vivo* remains uncertain (15, 21, 45, 63, 65, 66). Recent results from reconstitution of the regulation of $Ca_V1.2$ channels expressed in nonmuscle cells show that PKA phosphorylation of sites at the interface between the DCT and the proximal C terminus is responsible for regulation (19).

Although peak L-type $Ba^{2+}$ currents are much reduced in $DCT^{-/-}$ myocytes, these cells provide a unique experimental opportunity to examine the role of the DCT in regulation by the β-adrenergic/PKA pathway *in vivo*. Our results demonstrate for the first time in native cardiomyocytes that truncation of DCT abolishes the regulation of $Ca_V1.2$ channels by the β-adrenergic/PKA pathway. Deletion of the DCT also disrupts the expression and localization of AKAP15, which may contribute to impairment of PKA regulation. The requirement of the DCT for β-adrenergic stimulation of L-type $Ca^{2+}$ current is consistent with the hypothesis that β-adrenergic receptor/PKA signaling pathway acts through phosphorylation of sites at the interface between the proximal and distal C terminus, thereby relieving autoinhibition exerted by the cleaved, noncovalently associated DCT (18, 19).

In mammalian myocardium, $Ca_V1.2$ channels consist of three forms: full-length, truncated, and truncated channel with noncovalently associated DCT. Only ~20% is full-length channel (15). This proportion of channel forms provides a quantitative fit to the L-type $Ca^{2+}$ current in cardiac myocytes before and after treatment with isoproterenol if primarily the truncated channels with noncovalently bound DCT are up-regulated by PKA phosphorylation (18). Moreover, in recent studies, we have found that reconstitution of PKA regulation in nonmuscle cells requires formation of an autoinhibitory complex of truncated $Ca_V1.2$ channels with the noncovalently associated DCT and AKAP15 (19). These previous results are consistent with our current findings and support the conclusion that the DCT is required for β-adrenergic regulation of cardiac L-type $Ca^{2+}$ current. $DCT^{-/-}$ mice provide a unique model for study of the molecular mechanism of $Ca^{2+}$ channel regulation in the heart.

*Acknowledgments—The monoclonal antibody against $Ca_V1.2$ channels was developed by and obtained from the UC Davis/NIH NeuroMab Facility, supported by National Institutes of Health Grant U24NS050606 and maintained by the Department of Neurobiology, Physiology, and Behavior, College of Biological Sciences, University of California, Davis, CA 95616.*

## REFERENCES

1. Bers, D. M. (2000) *Circ. Res.* **87,** 275–281
2. Seisenberger, C., Specht, V., Welling, A., Platzer, J., Pfeifer, A., Kühbandner, S., Striessnig, J., Klugbauer, N., Feil, R., and Hofmann, F. (2000) *J. Biol. Chem.* **275,** 39193–39199
3. Moosmang, S., Schulla, V., Welling, A., Feil, R., Feil, S., Wegener, J. W., Hofmann, F., and Klugbauer, N. (2003) *EMBO J.* **22,** 6027–6034
4. Platzer, J., Engel, J., Schrott-Fischer, A., Stephan, K., Bova, S., Chen, H., Zheng, H., and Striessnig, J. (2000) *Cell* **102,** 89–97
5. Striessnig, J. (1999) *Cell. Physiol. Biochem.* **9,** 242–269
6. Catterall, W. A. (2000) *Annu. Rev. Cell Dev. Biol.* **16,** 521–555
7. Ertel, E. A., Campbell, K. P., Harpold, M. M., Hofmann, F., Mori, Y., Perez-Reyes, E., Schwartz, A., Snutch, T. P., Tanabe, T., Birnbaumer, L., Tsien, R. W., and Catterall, W. A. (2000) *Neuron* **25,** 533–535
8. Reuter, H. (1979) *Annu. Rev. Physiol.* **41,** 413–424
9. Hulme, J. T., Lin, T. W., Westenbroek, R. E., Scheuer, T., and Catterall, W. A. (2003) *Proc. Natl. Acad. Sci. U.S.A.* **100,** 13093–13098
10. Gray, P. C., Scott, J. D., and Catterall, W. A. (1998) *Curr. Opin. Neurobiol.* **8,** 330–334
11. Hulme, J. T., Ahn, M., Hauschka, S. D., Scheuer, T., and Catterall, W. A. (2002) *J. Biol. Chem.* **277,** 4079–4087
12. Hulme, J. T., Konoki, K., Lin, T. W., Gritsenko, M. A., Camp, D. G., 2nd, Bigelow, D. J., and Catterall, W. A. (2005) *Proc. Natl. Acad. Sci. U.S.A.* **102,** 5274–5279
13. De Jongh, K. S., Warner, C., Colvin, A. A., and Catterall, W. A. (1991) *Proc. Natl. Acad. Sci. U.S.A.* **88,** 10778–10782
14. De Jongh, K. S., Merrick, D. K., and Catterall, W. A. (1989) *Proc. Natl. Acad. Sci. U.S.A.* **86,** 8585–8589
15. De Jongh, K. S., Murphy, B. J., Colvin, A. A., Hell, J. W., Takahashi, M., and Catterall, W. A. (1996) *Biochemistry* **35,** 10392–10402
16. Wei, X., Neely, A., Lacerda, A. E., Olcese, R., Stefani, E., Perez-Reyes, E., and Birnbaumer, L. (1994) *J. Biol. Chem.* **269,** 1635–1640
17. Gao, T., Cuadra, A. E., Ma, H., Bunemann, M., Gerhardstein, B. L., Cheng, T., Ten Eick, R., and Hosey, M. M. (2001) *J. Biol. Chem.* **276,** 21089–21097
18. Hulme, J. T., Yarov-Yarovoy, V., Lin, T. W., Scheuer, T., and Catterall, W. A. (2006) *J. Physiol.* **576,** 87–102
19. Fuller, M. D., Emrick, M. A., Sadilek, M., Scheuer, T., and Catterall, W. A. (2010) *Sci. Signal.* **3,** ra70
20. Davies, M. P., An, R. H., Doevendans, P., Kubalak, S., Chien, K. R., and

Kass, R. S. (1996) *Circ. Res.* **78,** 15–25
21. Hulme, J. T., Westenbroek, R. E., Scheuer, T., and Catterall, W. A. (2006) *Proc. Natl. Acad. Sci. U.S.A.* **103,** 16574–16579
22. Snutch, T. P., Tomlinson, W. J., Leonard, J. P., and Gilbert, M. M. (1991) *Neuron* **7,** 45–57
23. Hell, J. W., Yokoyama, C. T., Wong, S. T., Warner, C., Snutch, T. P., and Catterall, W. A. (1993) *J. Biol. Chem.* **268,** 19451–19457
24. Westenbroek, R. E., Hell, J. W., Warner, C., Dubel, S. J., Snutch, T. P., and Catterall, W. A. (1992) *Neuron* **9,** 1099–1115
25. Gray, P. C., Johnson, B. D., Westenbroek, R. E., Hays, L. G., Yates, J. R., 3rd, Scheuer, T., Catterall, W. A., and Murphy, B. J. (1998) *Neuron* **20,** 1017–1026
26. Toyoshima, K., Momma, K., Imamura, S., and Nakanishi, T. (2006) *Biol. Neonate* **89,** 251–256
27. Brogden, R. N., and Sorkin, E. M. (1995) *Drugs* **49,** 618–649
28. Schachter, M. (1991) *J. Clin. Pharm. Ther.* **16,** 79–91
29. Momma, K., Toyoshima, K., Imamura, S., and Nakanishi, T. (2005) *Pediatr. Res.* **58,** 42–45
30. Luo, Z., Shyu, K. G., Gualberto, A., and Walsh, K. (1998) *Nat. Med.* **4,** 1092–1093
31. Sussman, M. A., Lim, H. W., Gude, N., Taigen, T., Olson, E. N., Robbins, J., Colbert, M. C., Gualberto, A., Wieczorek, D. F., and Molkentin, J. D. (1998) *Science* **281,** 1690–1693
32. Meguro, T., Hong, C., Asai, K., Takagi, G., McKinsey, T. A., Olson, E. N., and Vatner, S. F. (1999) *Circ. Res.* **84,** 735–740
33. Molkentin, J. D., Lu, J. R., Antos, C. L., Markham, B., Richardson, J., Robbins, J., Grant, S. R., and Olson, E. N. (1998) *Cell* **93,** 215–228
34. Bezanilla, F. (2000) *Physiol. Rev.* **80,** 555–592
35. Hadley, R. W., and Lederer, W. J. (1991) *J. Gen. Physiol.* **98,** 265–285
36. Hadley, R. W., and Lederer, W. J. (1992) *Am. J. Physiol.* **262,** H472–H477
37. Brunet, S., Scheuer, T., and Catterall, W. A. (2009) *J. Gen. Physiol.* **134,** 81–94
38. Hulme, J. T., Scheuer, T., and Catterall, W. A. (2004) *J. Mol. Cell. Cardiol.* **37,** 625–631
39. Bünemann, M., Gerhardstein, B. L., Gao, T., and Hosey, M. M. (1999) *J. Biol. Chem.* **274,** 33851–33854
40. Tsien, R. W., Bean, B. P., Hess, P., Lansman, J. B., Nilius, B., and Nowycky, M. C. (1986) *J. Mol. Cell Cardiol.* **18,** 691–710
41. An, R. H., Davies, M. P., Doevendans, P. A., Kubalak, S. W., Bangalore, R., Chien, K. R., and Kass, R. S. (1996) *Circ. Res.* **78,** 371–378
42. Kamp, T. J., and Hell, J. W. (2000) *Circ. Res.* **87,** 1095–1102
43. Gao, T., Puri, T. S., Gerhardstein, B. L., Chien, A. J., Green, R. D., and Hosey, M. M. (1997) *J. Biol. Chem.* **272,** 19401–19407
44. Steinberg, S. F. (2004) *J. Mol. Cell. Cardiol.* **37,** 407–415
45. Gao, T., Yatani, A., Dell'Acqua, M. L., Sako, H., Green, S. A., Dascal, N., Scott, J. D., and Hosey, M. M. (1997) *Neuron* **19,** 185–196
46. Deedwania, P. C. (1997) *Am. J. Hypertens.* **10,** 280S–288S
47. Hansson, L., Lindholm, L. H., Niskanen, L., Lanke, J., Hedner, T., Niklason, A., Luomanmäki, K., Dahlöf, B., de Faire, U., Mörlin, C., Karlberg, B. E., Wester, P. O., and Björck, J. E. (1999) *Lancet* **353,** 611–616
48. Anderson, J. R., and Nawarskas, J. J. (2010) *Cardiol. Rev.* **18,** 148–162
49. Schulla, V., Renström, E., Feil, R., Feil, S., Franklin, I., Gjinovci, A., Jing, X. J., Laux, D., Lundquist, I., Magnuson, M. A., Obermüller, S., Olofsson, C. S., Salehi, A., Wendt, A., Klugbauer, N., Wollheim, C. B., Rorsman, P., and Hofmann, F. (2003) *EMBO J.* **22,** 3844–3854
50. Moosmang, S., Haider, N., Klugbauer, N., Adelsberger, H., Langwieser, N., Müller, J., Stiess, M., Marais, E., Schulla, V., Lacinova, L., Goebbels, S., Nave, K. A., Storm, D. R., Hofmann, F., and Kleppisch, T. (2005) *J. Neurosci.* **25,** 9883–9892
51. Fernández-Tenorio, M., González-Rodríguez, P., Porras, C., Castellano, A., Moosmang, S., Hofmann, F., Ureña, J., and López-Barneo, J. (2010) *Circ. Res.* **106,** 1285–1289
52. Hescheler, J., and Trautwein, W. (1988) *J. Physiol.* **404,** 259–274
53. Mikala, G., Bodi, I., Klockner, U., Varadi, M., Varadi, G., Koch, S. E., and Schwartz, A. (2003) *Mol. Cell. Biochem.* **250,** 81–89
54. Piacentino, V., 3rd, Weber, C. R., Chen, X., Weisser-Thomas, J., Margulies, K. B., Bers, D. M., and Houser, S. R. (2003) *Circ. Res.* **92,** 651–658
55. Beuckelmann, D. J., and Erdmann, E. (1992) *Basic Res. Cardiol.* **87,** 235–243
56. Gómez, A. M., Valdivia, H. H., Cheng, H., Lederer, M. R., Santana, L. F., Cannell, M. B., McCune, S. A., Altschuld, R. A., and Lederer, W. J. (1997) *Science* **276,** 800–806
57. Chen, X., Piacentino, V., 3rd, Furukawa, S., Goldman, B., Margulies, K. B., and Houser, S. R. (2002) *Circ. Res.* **91,** 517–524
58. Gomez-Ospina, N., Tsuruta, F., Barreto-Chang, O., Hu, L., and Dolmetsch, R. (2006) *Cell* **127,** 591–606
59. Schroder, E., Byse, M., and Satin, J. (2009) *Circ. Res.* **104,** 1373–1381
60. Sperelakis, N., and Schneider, J. A. (1976) *Am. J. Cardiol.* **37,** 1079–1085
61. Reuter, H., and Scholz, H. (1977) *J. Physiol.* **264,** 17–47
62. Tsien, R. W., Giles, W., and Greengard, P. (1972) *Nat. New Biol.* **240,** 181–183
63. Ganesan, A. N., Maack, C., Johns, D. C., Sidor, A., and O'Rourke, B. (2006) *Circ. Res.* **98,** e11–18
64. Norman, R. I., and Leach, R. N. (1994) *Biochem. Soc. Trans.* **22,** 492–496
65. Mitterdorfer, J., Froschmayr, M., Grabner, M., Moebius, F. F., Glossmann, H., and Striessnig, J. (1996) *Biochemistry* **35,** 9400–9406
66. Lemke, T., Welling, A., Christel, C. J., Blaich, A., Bernhard, D., Lenhardt, P., Hofmann, F., and Moosmang, S. (2008) *J. Biol. Chem.* **283,** 34738–34744